

Short communication

# High-performance low-temperature solid oxide fuel cell with novel BSCF cathode

Q.L. Liu\*, K.A. Khor, S.H. Chan

*Fuel Cell Strategic Research Programme, School of Mechanical and Aerospace Engineering,  
Nanyang Technological University, Singapore 639798, Singapore*

Received 10 January 2006; accepted 20 March 2006

Available online 23 June 2006

## Abstract

An anode-supported solid oxide fuel cell (SOFC), consisting of a dense  $10\ \mu\text{m}$   $\text{Gd}_{0.1}\text{Ce}_{0.9}\text{O}_{1.95}$  (GDC) electrolyte, a porous  $\text{Ba}_{0.5}\text{Sr}_{0.5}\text{Co}_{0.8}\text{Fe}_{0.2}\text{O}_{3-\delta}$  (BSCF) cathode and a porous Ni–GDC cermet anode, is successfully assembled and electrochemically characterized. With humidified (3% water vapour) hydrogen as the fuel and air as the oxidant, the cell exhibits open-circuit voltages of 0.903 and 0.984 V when operating at 600 and 500 °C, respectively. The cell produces peak power densities of 1329, 863, 454, 208 and 83  $\text{mW cm}^{-2}$  at 600, 550, 500, 450 and 400 °C, respectively. These results are impressive and demonstrate the potential of BSCF for use as the cathode material in new-generation SOFCs with GDC as the electrolyte. In addition, the sustained performance at temperatures below 600 °C warrants commercial exploitation of this SOFC in stationary and mobile applications.

© 2006 Elsevier B.V. All rights reserved.

**Keywords:** Solid oxide fuel cell; Low-temperature; Anode-supported; Novel BSCF cathode; Gadolinia-doped ceria electrolyte; Power density

## 1. Introduction

The attraction of solid oxide fuel cells (SOFC) is based on a number of aspects that include the clean conversion of chemical energy to electricity, low levels of noise pollution, the ability to operate with different fuels, but most of all—high efficiency [1]. The enhanced efficiency of the SOFC in comparison with other energy-conversion systems is due to its high operating temperature, which in some designs may exceed 1000 °C. Operating the SOFC at high temperatures is, however, associated with high material costs, in particular for the interconnect and the construction materials. In high-temperature SOFCs, the interconnect may be a ceramic such as lanthanum chromite, or, if the temperature is limited to <1000 °C, a sophisticated refractory alloy, for example, based on mechanically alloyed Y/Cr. In either case, the interconnect represents a major proportion of the cost of the stack [2]. Stack construction materials and the balance-of-plant also need to be refractory to contain and manipulate the high-temperature gas streams. In addition, a drawback to the use of

chromium-containing ceramics and alloys is the volatility of the material that can result in contamination of the stack components [2]. This has an increased significance for future reclamation of materials and components from used stacks where the presence of a toxic material such as  $\text{Cr}^{6+}$  would require special disposal procedures.

By contrast, reducing the operating temperature of the SOFC to less than 650 °C would have the following advantages:

- Offer the choice of low-cost metallic materials such as ferritic stainless-steels for the interconnect and construction materials. This makes both the stack and balance-of-plant cheaper and more robust. It also significantly reduces the above-mentioned problems associated with chromium.
- Offer the potential for more rapid start-up and shut-down procedures.
- Simplify the design and materials requirements of the balance-of-plant.
- Significantly reduce the corrosion rates.

Unfortunately, conventional SOFCs based on yttria-stabilized zirconia (YSZ) electrolyte, strontium-doped lanthanum (LSM) cathode and Ni–YSZ cermet anode have to operate

\* Corresponding author. Tel.: +65 6790 5571; fax: +65 6792 4062.  
E-mail address: [qliu@ntu.edu.sg](mailto:qliu@ntu.edu.sg) (Q.L. Liu).

in high temperature range of 900–1000 °C to achieve desired performance characteristics. The high operating temperature of conventional SOFCs has imposed stringent material and processing requirements (implication of high cost), which prevent SOFCs from commercialization. Therefore, it is quite desirable to operate SOFCs at intermediate temperatures (600–800 °C) which allow a broader choice of materials for interconnects and manifolds, including inexpensive metal alloys, as well as decreasing electrode sintering and minimizing the interfacial diffusion between the electrolyte and the electrode. In addition, for potential applications in transportation that involve frequent thermal cycling and rapid start-up, the operating temperature is expected to be decreased further to around 500 °C [3].

To lower the SOFC operating temperature, research and development have focused on the following approaches: (i) decrease of YSZ electrolyte thickness [4–6]; (ii) adoption of alternative electrolyte materials with higher ionic conductivity at low temperatures than conventional YSZ, such as doped ceria and doped lanthanum gallate [7–10]; (iii) minimization of electrode polarization resistance [11–13]. Meanwhile, many techniques have been developed for thin-film electrolyte fabrication to reduce the electrolyte resistance [14]. Considerable progress has been made in the study of low-temperature SOFCs based on a thin-film electrolyte of doped ceria, mainly gadolium-doped ceria (GDC), in combination with various cathode materials which present much better performance than LSM [3,15–19]. Doshi et al. [3] applied a multilayer tape-casting technique to assemble a fuel cell that consisted of a 30 μm thick Gd<sub>0.2</sub>Ce<sub>0.8</sub>O<sub>1.9</sub> (GDC) electrolyte, a Ni–GDC anode, and an ANLC-1 cathode. The cell generated a peak power density of 140 mW cm<sup>-2</sup> at 500 °C when using hydrogen and air. Xia and Liu [16] developed a dry-pressing technique to prepare electrolyte films based on foam-like Gd<sub>0.1</sub>Ce<sub>0.9</sub>O<sub>1.95</sub> (GDC) powders. The cell, assembled with a Sm<sub>0.5</sub>Sr<sub>0.5</sub>O<sub>3-δ</sub> (SSC)–GDC cathode and a 20 μm thick GDC electrolyte supported on a Ni–GDC cermet anode, exhibited maximum power densities of 145 and 400 mW cm<sup>-2</sup> at 500 and 600 °C, respectively. Comparatively, Leng et al. [17] substantially improved the performance of GDC-based cells, which at 600 °C gave a maximum power density of 578 mW cm<sup>-2</sup>. The cell used a 10 μm thin-film Gd<sub>0.2</sub>Ce<sub>0.8</sub>O<sub>1.9</sub> (GDC) electrolyte and was prepared by a spray-coating method with a Ni–GDC anode substrate and a La<sub>0.8</sub>Sr<sub>0.2</sub>Co<sub>0.2</sub>Fe<sub>0.8</sub>O<sub>3-δ</sub> (LSCF)–GDC composite cathode. The cell, however, demonstrated a similar performance to the above-mentioned cells, i.e. a peak power density of 167 mW cm<sup>-2</sup> at 500 °C. This performance is still far from the forecast given by Steele [18], i.e. a peak power density of ~400 mW cm<sup>-2</sup> at 500 °C with a 25 μm thin film Gd<sub>0.1</sub>Ce<sub>0.9</sub>O<sub>1.95</sub> electrolyte and an electrode (both anode and cathode) area specific resistance of  $R_a = R_c = 0.2 \Omega \text{ cm}^2$  [18]. In fact, when the operating temperature is lowered to around 500 °C, the electrode overpotentials, mainly the cathode overpotential, dominate the overall cell performance. Consequently, efforts have to be directed towards improvement of cathode performance and development of novel cathode materials in order to achieve the power density anticipated by Steele for the GDC-based SOFCs [19,20].

Recently, Shao and Haile [21] reported a new cathode material, Ba<sub>0.5</sub>Sr<sub>0.5</sub>Co<sub>0.8</sub>Fe<sub>0.2</sub>O<sub>3-δ</sub> (BSCF) for low-temperature SOFCs, which has been extensively investigated as an oxygen permeation membrane material for oxygen generation [22]. With this BSCF cathode, outstanding performance has been obtained at low temperatures from a single cell based on a 20 μm thick Sm<sub>0.15</sub>Ce<sub>0.85</sub>O<sub>1.925</sub> (SDC) electrolyte film. Maximum power densities of 1010 and 402 mW cm<sup>-2</sup> were produced at 600 and 500 °C, respectively. To the author's knowledge, no other publication is available on the BSCF cathode. As this material is a potential candidate for low-temperature SOFC development, extensive and detailed studies on BSCF cathodes are necessary in terms of the oxygen reduction reaction mechanism, phase stability, compatibility with other doped CeO<sub>2</sub> or doped LaGaO<sub>3</sub> materials, as well as long-term performance stability in a practical SOFC operating environment. According to Steele [18], Gd<sub>2</sub>O<sub>3</sub> is the preferred dopant for CeO<sub>2</sub> oxide compared with Sm<sub>2</sub>O<sub>3</sub> and Y<sub>2</sub>O<sub>3</sub> because (Gd<sup>4+</sup>–V<sub>O</sub><sup>••</sup>) complexes exhibit the lowest association enthalpy and Gd<sub>2</sub>O<sub>3</sub>-doped CeO<sub>2</sub> has a much better ionic conductivity at low temperatures. Therefore, it is of importance and significance to examine the performance of BSCF/GDC systems.

This study presents the fabrication and characterization of thin-film GDC cells with BSCF cathodes. The results demonstrate the successful incorporation of BSCF cathodes into GDC-based cells, which constitutes significant progress in the development of low-temperature SOFCs.

## 2. Experimental

Fabrication of the anode-supported thin-film GDC electrolyte cell began with the preparation of bilayers of GDC electrolyte film on a porous anode substrate via a modified dry-pressing process, i.e. a spray-copressing method. The anode powder was prepared by ball-milling NiO powder (J.T. Baker, US) and nano-sized Gd<sub>0.1</sub>Ce<sub>0.9</sub>O<sub>1.95</sub> powder (Nextech, US) in a composition ratio of 65 to 35 by weight. The resulting NiO–GDC mixture was then uniaxially pressed at 100 MPa with a steel die of 24 mm diameter. To prepare the electrolyte film on the anode, a suspension of GDC (GDC powder dispersed uniformly in alcohol with some additives) was sprayed onto the pre-pressed green NiO–GDC substrate, which was contained in the die. After the solvent was evaporated, the GDC powder and the anode substrate were co-pressed under a pressure of 250 MPa to form a green bilayer. The bilayer was co-sintered at 1300 °C for 4 h in a furnace to become a dense electrolyte film with a diameter of ~20 mm and a thickness of ~0.8 mm.

The cathode material Ba<sub>0.5</sub>Sr<sub>0.5</sub>Co<sub>0.8</sub>Fe<sub>0.2</sub>O<sub>3-δ</sub> (BSCF) was synthesized by a sol–gel process in which appropriate amounts of various metal nitrates were dissolved in distilled water, and a combination of EDTA and citric acid served as complexing agents [22]. Gelation of the solution took place on the evaporation of water. The gel was then heat-treated at 135 °C for 5 h to produce a primary powder, which was subsequently calcined at 800 °C for 2 h to form the final powder. The crystal structure of the synthesized BSCF powder was examined with an X-ray diffractometer (Philips MPD1880) using monochromatic

Cu  $K\alpha_1$  radiation generated at 40 kV and 30 mA. To prepare the cathode, BSCF powder was mixed with polyethylene glycol 400 and the resultant paste was painted on the centre of the electrolyte side of electrolyte–anode bilayer to give a cathode area of  $0.5 \text{ mm}^2$ . The electrode was then sintered at  $950^\circ\text{C}$  for 2 h. To minimize the contact resistance between the cathode and the Pt mesh, Pt paste was painted on the cathode surface to serve as a current-collector. The assembly was then sintered at  $900^\circ\text{C}$  for 30 min.

The cell performance was evaluated using an in-house SOFC test station. The anode side of the cell was sealed with a ceramic paste. During the course of testing, humidified hydrogen (3% water vapour) was fed to the anode chamber at a flow rate of 70 sccm, while the cathode was exposed to an air flow at 350 sccm. The NiO in the anode was reduced to Ni in situ in the hydrogen atmosphere. Electrochemical measurements were performed with a four-lead two-electrode configuration using Autolab PG30/FRA equipment combined with a 10 A current booster (Eco Chimie, The Netherlands). The current–voltage characteristics of the cell were determined by linear sweep voltammetry at intervals of  $50^\circ\text{C}$  over a temperature range of  $600\text{--}400^\circ\text{C}$ . The overall cell impedance was measured in the frequency window of 100 kHz to 0.01 Hz with an amplitude of 10 mV under open-circuit conditions. After testing, the microstructure of the cell was examined by means of scanning electron microscopy (SEM, Leica 360).

### 3. Results and discussion

The X-ray diffraction (XRD) pattern of the synthesized BSCF powder after calcination at  $800^\circ\text{C}$  for 2 h is given in Fig. 1. All the peaks are well indexed as a cubic perovskite structure,

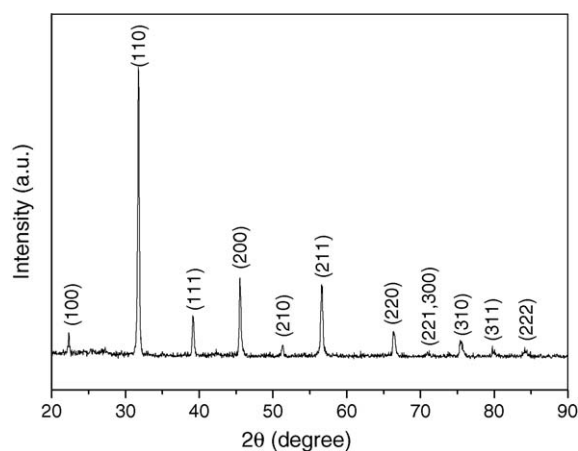


Fig. 1. XRD pattern of BSCF powder after calcination at  $800^\circ\text{C}$  for 2 h.

and sharp lines reflect a well-developed crystallization. These features indicate that a single crystalline phase of BSCF oxide is successfully obtained after calcination.

To minimize the electrolyte resistance at low-temperature operation, great efforts have been made to fabricate GDC-based anode-supported cells by a spray-copressing method, as described above. After electrochemical testing of a single anode-supported cell that consists of a GDC electrolyte, a BSCF cathode and a Ni–GDC cermet anode, cross-sectional micrographs show that the GDC electrolyte film is about  $10 \mu\text{m}$  thick and is sandwiched by a porous cathode (top layer) and a porous anode (bottom layer) (see Fig. 2(a)). Good adhesion can also be seen at both the cathode|electrolyte and anode|electrolyte interfaces, which has been produced by high temperature firing. The dense structure of the electrolyte film can be seen clearly in Fig. 2(b).

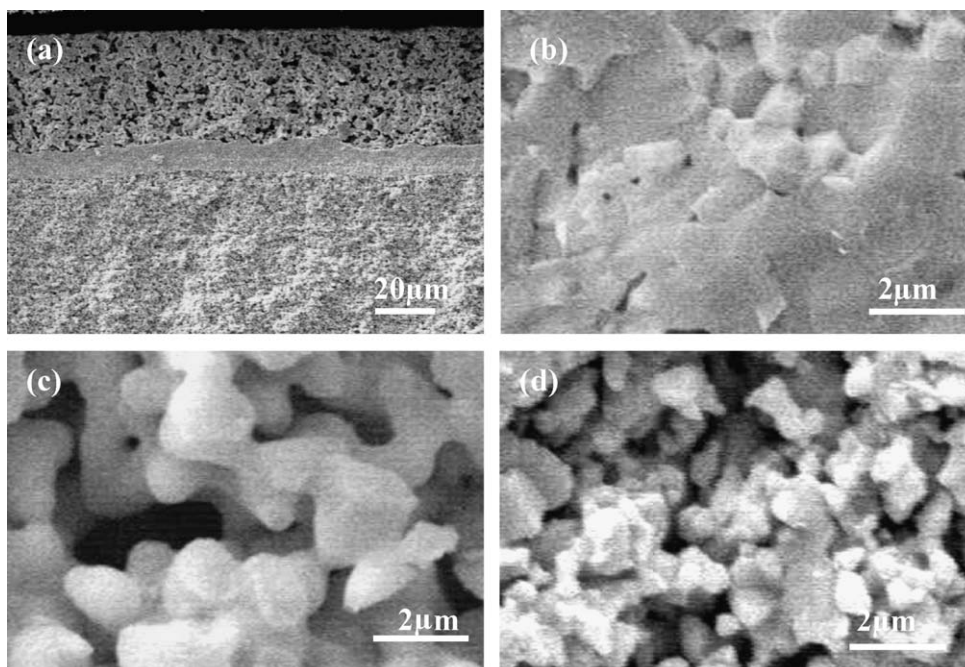


Fig. 2. Cross-sectional scanning electron micrographs of anode-supported cell: (a) entire cell at low magnification (top layer: cathode; middle layer: electrolyte; bottom layer: anode support); (b) GDC electrolyte; (c) BSCF cathode; (d) Ni–GDC anode at higher magnification.

The GDC film seems almost fully dense except a few isolated voids, and no cross-film cracks or pinholes are observed. This morphology shows that the 10  $\mu\text{m}$  thick GDC electrolyte film has been successfully fabricated onto the anode substrate by the spray-copressing method developed in-house. In contrast to the dense electrolyte film, both the cathode (Fig. 2(c)) and the anode (Fig. 2(d)) are highly porous. Sufficient porosity is important for electrodes in order to allow rapid transport of gaseous reactants and to provide abundant sites for electrochemical reactions in properly designed electrodes. It is noted that the BSCF cathode has a much coarser structure than the Ni–GDC anode, though the former was sintered at much lower temperature than the latter (950 versus 1300  $^{\circ}\text{C}$ ). This indicates that the BSCF powder exhibits a much higher sinterability than the NiO–GDC powder. It is reasonable to conclude that refining and optimizing the cathode microstructure will improve the electrochemical activity of the BSCF electrode.

The voltages and the corresponding power densities are expressed in Fig. 3 as a function of current density for a single cell (as in Fig. 2), measured with humidified hydrogen and air at temperatures from 400 to 600  $^{\circ}\text{C}$ . An open-circuit voltage (OCV) of 0.903 V is recorded at 600  $^{\circ}\text{C}$ . This is 40 mV higher than that of the cell reported by Leng et al. [17] that had a GDC electrolyte with the same thickness. This implies that a dense electrolyte film has been successfully achieved in this study and is consistent with the microstructural observation (Fig. 2(b)). The OCV value, however, still displays a large deviation from the theoretical value, i.e. 1.138 V at 600  $^{\circ}\text{C}$ , which is due to the electronic conductivity of doped-ceria materials induced by the reduction of  $\text{Ce}^{4+}$  to  $\text{Ce}^{3+}$  in reducing atmospheres [23,24]. This loss in OCV can be partly alleviated as the temperature decreases. At 500 and 400  $^{\circ}\text{C}$ , the cell produces an OCV of 0.984 and 1.032 V, respectively. These voltages are much closer to the theoretical value and suggests that the electronic conductivity of the GDC electrolyte is insignificant at these low temperatures. This implicitly demonstrates that doped ceria is a very promising candidate electrolyte for use in SOFCs, in particular those operating at around 500  $^{\circ}\text{C}$  [18].

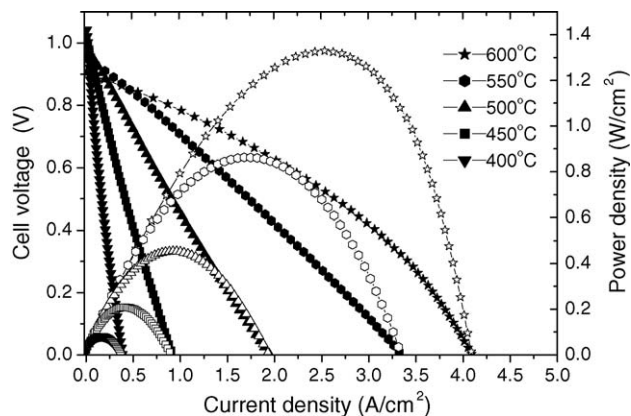


Fig. 3. Cell voltages (solid symbols) and power densities (open symbols) as function of current density of anode-supported cell, consisting of 10  $\mu\text{m}$  GDC electrolyte, BSCF cathode and Ni–GDC anode; measured in humidified hydrogen and air in temperature range of 400–600  $^{\circ}\text{C}$ .

As seen in Fig. 3, the cell voltage versus current density measured at 600  $^{\circ}\text{C}$  exhibits a downward bending curve at higher current densities, which is obviously different from the polarization behaviour observed at temperatures below 600  $^{\circ}\text{C}$ . This is typical diffusion polarization behaviour that arises from a limited supply of reactants. To verify if hydrogen or air was insufficiently supplied, the effects of air and hydrogen flow rates on the polarization behaviour of the cell were examined at 600  $^{\circ}\text{C}$ . The limiting current density increases with increase in the hydrogen flow rate and but does not change noticeably with increase in the airflow rate. These characteristics demonstrate that the observed diffusion polarization is due to hydrogen diffusion limitations at the anode. The microstructure of the anode shown in Fig. 2(d) reveals that, though with good porosity, the relatively thick anode of 0.8 mm, which serves as the cell support in this study, is probably the cause of diffusion limitations. The diffusion polarization caused by limited hydrogen supply can be overcome by adopting a reduction in the anode substrate thickness [3,4] and/or by applying a double-layer anode structure with thin functional anode layer on top of an anode substrate of enhanced porosity [25].

With humidified hydrogen as fuel and air as oxidant, the present cell generates maximum power densities of 1329, 863, 454, 208 and 83  $\text{mW}/\text{cm}^2$  at low temperatures from 600 down to 400  $^{\circ}\text{C}$  at intervals of 50  $^{\circ}\text{C}$ . These results are impressive and, to our knowledge, represent the best performance ever reported for low-temperature SOFCs. For comparison, the maximum power densities at the different temperatures employed in this study are plotted in Fig. 4 against other results obtained from the literature with different cathode materials. Cells with BSCF cathodes present much higher power outputs than those with other cathode materials, namely: LSCF–GDC [17], SSC–GDC [16], ANLC-1 [3] and Ag-BICUVOX [19]. At 500  $^{\circ}\text{C}$ , for example, the maximum power density is 454  $\text{mW}/\text{cm}^2$  for the cell with the BSCF cathode used in this study is about three times that of cells with cathodes of LSCF–GDC, SSC–GDC and ANLC-1, i.e. 167, 145 and 140  $\text{mW}/\text{cm}^2$ , respectively, and is almost double the performance of the cell with a novel Ag-BICUVOX cathode, i.e.

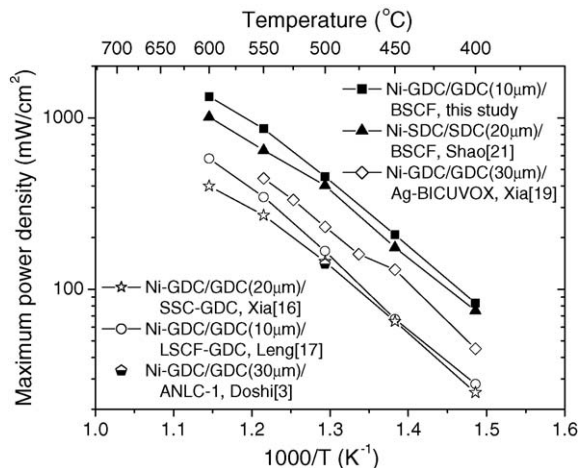


Fig. 4. Comparison of maximum power densities of thin-film GDC or SDC electrolyte cells with various cathodes.

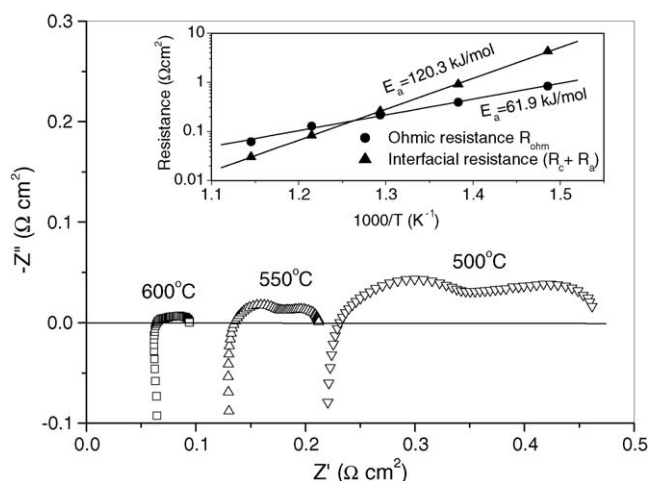


Fig. 5. Impedance spectra of cell consisting of 10  $\mu\text{m}$  GDC electrolyte, BSCF cathode and Ni–GDC anode; measured under open-circuit conditions at 500, 550 and 600  $^{\circ}\text{C}$ , respectively. Inset shows Arrhenius plots of ohmic resistance  $R_{\text{ohm}}$  and total interfacial polarization resistance ( $R_a + R_c$ ).

231  $\text{mW cm}^{-2}$  [19]. Hence, with the introduction of the BSCF cathode, a significant improvement in power output has been achieved from doped ceria electrolyte cells operating at low temperatures. It is noted that the cell based on a 10  $\mu\text{m}$  GDC thin-film electrolyte and a BSCF cathode has produced greater power densities at low temperature than that based on the same BSCF cathode but with a thicker SDC electrolyte film of 20  $\mu\text{m}$  [21]. At 600  $^{\circ}\text{C}$ , the maximum power density of the former is 1329  $\text{mW cm}^{-2}$ , which is much higher than 1010  $\text{mW cm}^{-2}$  for the latter. The improved power output is attributed to the use of a thinner electrolyte.

Impedance spectra for the fuel cell with a two-electrode configuration measured at 500, 550 and 600  $^{\circ}\text{C}$  under open-circuit conditions are given in Fig. 5. The ohmic resistance  $R_{\text{ohm}}$  and the total interfacial polarization resistance (i.e. the anode|electrolyte interfacial polarization resistance  $R_a$  and the cathode|electrolyte interfacial polarization resistance  $R_c$ ) of the cell were extracted by fitting the impedance spectra to an equivalent circuit with a configuration of  $LR_{\text{ohm}}(RQ)_{\text{HF}}(RQ)_{\text{LF}}$ , where  $L$  is an inductance,  $R$  a resistance,  $Q$  a constant phase element, and the subscripts represent the respective high- and low-frequency contribution. The extracted results are shown as an inset in Fig. 5 in the form of Arrhenius plots. Obviously, the ohmic resistance dominates the total cell resistance at temperatures above 500  $^{\circ}\text{C}$ , while the interfacial polarization resistance of the electrodes controls the total cell resistance at temperatures below 500  $^{\circ}\text{C}$ . From the slopes of the Arrhenius plots, apparent activation energies of 120.3 and 61.9  $\text{kJ mol}^{-1}$  are determined for the ohmic resistance and the total interfacial polarization resistance, respectively. The activation energy for the total interfacial polarization resistance of the cell is very close to 116  $\text{kJ mol}^{-1}$ , which is the activation energy for the interfacial polarization resistance of BSCF cathode on SDC electrolyte as reported by Shao and Haile [21]. It appears that the cathode|electrolyte interfacial polarization resistance dominates the total interfacial polarization resistance of the cell within the range of temperatures under investigation.

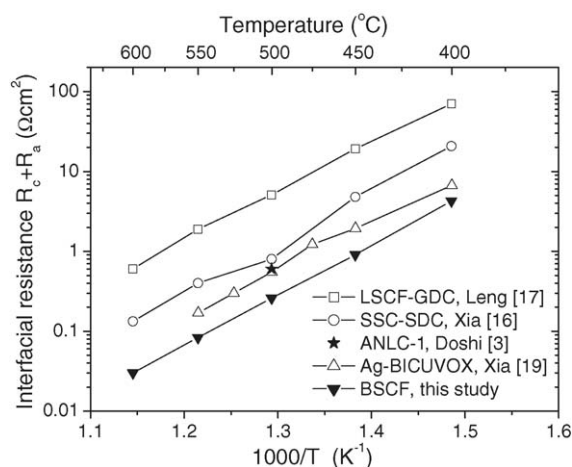


Fig. 6. Comparison of total interfacial resistance ( $R_a + R_c$ ) of thin-film GDC electrolyte cells with various cathodes indicated in legend.

The fuel cell developed in this study displays a much lower total interfacial resistance than those reported with other cathode materials (Fig. 6). For example, at 500  $^{\circ}\text{C}$ , the total interfacial resistance is 5.1, 0.763,  $\sim 0.6$ , 0.55 and 0.26  $\Omega \text{cm}^{-2}$  for SOFCs with LSCF–GDC [17], SSC–GDC [16], ANLC-1 [3], Ag-BICUVOX [19] and BSCF cathodes, respectively. Given that the anodes of the five cells are basically the same and that the anode|electrolyte interfacial polarization resistance is negligible [3,16,19], the difference between the total interfacial polarization resistance values of the five cells is attributed to the use of different cathode materials. Among these five GDC-based cells, the cell with BSCF cathode prepared in this study exhibits the lowest total interfacial polarization resistance, which well explains the excellent cell performance shown in Fig. 4.

#### 4. Conclusions

Dense and crack-free GDC electrolyte films have been successfully fabricated on anode substrates by a modified dry-pressing process, i.e. spray-copressing, after co-sintering at 1300  $^{\circ}\text{C}$ . BSCF powders are synthesized via a sol–gel approach, and the resultant powders have a single crystalline, solid-solution, phase structure after being calcined at 800  $^{\circ}\text{C}$ . An anode-supported SOFC based on a 10  $\mu\text{m}$  GDC electrolyte film has been assembled, using the BSCF material as cathode, and tested at low temperatures with humidified (3% water vapour) hydrogen and air as the feedstocks. An OCV of 0.903 and 0.984 V is recorded at 600 and 500  $^{\circ}\text{C}$ , respectively. Maximum power densities of 1329, 863, 454, 208 and 83  $\text{mW cm}^{-2}$  are obtained when the cell is operated at 600, 550, 500, 450 and 400  $^{\circ}\text{C}$ , respectively. Compared with thin-film GDC electrolyte cells with LSCF-based and SSC-based cathodes, the cell with a BSCF cathode shows a much lower interfacial polarization resistance at low temperatures. Although the long-term stability of the BSCF cell has yet to be evaluated, the obtained power outputs are encouraging and indicate a new generation of low-temperature SOFCs could become a reality.

## References

- [1] N.Q. Minh, *J. Am. Ceram. Soc.* 76 (1993) 563.
- [2] S.C. Singhal, K. Kendall, *High Temperature Solid Oxide Fuel Cells: Fundamentals, Design and Applications*, Elsevier Advanced Technology, UK, 2003.
- [3] R. Doshi, V.L. Richards, J.D. Carter, X. Wang, M. Krumpelt, *J. Electrochem. Soc.* 146 (1999) 1273.
- [4] S. de Souza, S.J. Visco, L.C. de Jonghe, *Solid State Ionics* 98 (1997) 57.
- [5] T. Tsai, S.A. Barnett, *Solid State Ionics* 98 (1997) 191.
- [6] J.W. Kim, A.V. Virkar, K.Z. Fung, K. Mehta, S.C. Singhal, *J. Electrochem. Soc.* 146 (1999) 69.
- [7] T. Ishihara, T. Shibayama, M. Honda, H. Nishiguchi, Y. Takita, *J. Electrochem. Soc.* 147 (2000) 1332.
- [8] J.W. Yan, Z.G. Lu, Y. Jiang, Y.L. Dong, C.Y. Yu, W.Z. Li, *J. Electrochem. Soc.* 149 (2002) A1132.
- [9] T. Fukui, S. Ohara, K. Murata, H. Yoshida, K. Miura, T. Inagaki, *J. Power Sources* 106 (2002) 142.
- [10] K. Huang, J.H. Wan, J.B. Goodenough, *J. Electrochem. Soc.* 148 (2001) A788.
- [11] S.P. Jiang, Y.L. Leng, S.H. Chan, K.A. Khor, *Electrochem. Solid-State Lett.* 6 (2003) A67.
- [12] V. Dusastre, J.A. Kilner, *Solid State Ionics* 126 (1999) 163.
- [13] C. Xia, W. Rauch, F. Chen, M. Liu, *Solid State Ionics* 149 (2002) 11.
- [14] J. Will, A. Mitterdorfer, C. Kleinlogel, D. Perednis, L.J. Gauckler, *Solid State Ionics* 131 (2000) 79.
- [15] K. Zheng, B.C.H. Steele, M. Sahibzada, I.S. Metcalfe, *Solid State Ionics* 86–88 (1996) 1241.
- [16] C. Xia, M. Liu, *Solid State Ionics* 144 (2001) 249.
- [17] Y.J. Leng, S.H. Chan, S.P. Jiang, K.A. Khor, *Solid State Ionics* 170 (2004) 9.
- [18] B.C.H. Steele, *Solid State Ionics* 129 (2000) 95.
- [19] C. Xia, M. Liu, *Adv. Mater.* 14 (2002) 521.
- [20] Y. Liu, S. Zha, M. Liu, *Adv. Mater.* 16 (2004) 256.
- [21] Z.P. Shao, S.M. Haile, *Nature (London)* 431 (2004) 170.
- [22] Z.P. Shao, W.S. Yang, Y. Cong, H. Dong, J.H. Tong, G.X. Xiong, *J. Membr. Sci.* 172 (2000) 177.
- [23] S.P.S. Badwal, F.T. Ciacchi, J. Drennan, *Solid State Ionics* 121 (2001) 253.
- [24] M. Mogensen, N.M. Sammes, G.A. Tompsett, *Solid State Ionics* 129 (2000) 63.
- [25] Y. Jiang, A.V. Virkar, *J. Electrochem. Soc.* 148 (2001) A706.